Proc. Natl. Acad. Sci. USA
Vol. 90, pp. 8053–8057, September 1993
Immunology

Comparison of the P2 specificity pocket in three human histocompatibility antigens: HLA-A*6801, HLA-A*0201, and HLA-B*2705

(protein crystal structure/allelic specificity/peptide binding/antigen presentation)

H.-C. GUO†, D. R. MADDEN†, M. L. SILVER†‡, T. S. JARDETZKY†, J. C. GORGA†§, J. L. STROMINGER†, AND D. C. WILEY†¶‖

†Department of Biochemistry and Molecular Biology, Harvard University, and ¶Howard Hughes Medical Institute, 7 Divinity Avenue, Cambridge MA 02138

Contributed by D. C. Wiley, June 4, 1993

ABSTRACT **Coordinates from x-ray structures of HLA-A*6801, HLA-A*0201, and HLA-B*2705 were analyzed to examine the basis for their selectivity in peptide binding. The pocket that binds the side chain of the peptide's second amino acid residue (P2 residue) shows a preference for Val, Leu, and Arg in these three HLA subtypes, respectively. The Arg-specific pocket of HLA-B*2705 differs markedly from those of HLA-A*0201 and HLA-A*6801, as a result of numerous differences in the side chains that form the pocket's surface. The cause of the specificity differences between HLA-A*0201 and HLA-A*6801 is more subtle and depends both on a change in conformation of pocket residue Val-67 and on a sequence difference at residue 9. The Val-67 conformational change appears to be caused by a shift in the position of the α_1-domain α-helix relative to the β-sheet in the cleft and may, in fact, depend on amino acid differences remote from the P2 pocket. Analysis of the stereochemistry of the P2 side chain interacting with its binding pocket permits an estimate to be made of its contribution to the free-energy change of peptide binding.**

Class I histocompatibility antigens bind short peptides, usually nonamers (1), derived from proteins expressed inside a cell (2) and "present" them for recognition by T-cell receptors on cytotoxic T lymphocytes, as part of a surveillance mechanism for detecting foreign antigens (3). The class I isotypes, HLA-A, -B, and -C, are encoded at three loci within the human major histocompatibility complex (MHC) and many alleles are known for each locus (4). Each subtype of HLA preferentially binds peptides with certain amino acids ("anchors") at specific positions along the peptide, often near the termini—e.g., at peptide position 2 (P2), P3, or PΩ (where Ω is the C-terminal peptide position) (5–8). The three-dimensional structures of collections of endogenous human peptides complexed with three subtypes of HLA (8–11) and three single viral peptides complexed with class I molecules (12–15) have been determined by x-ray crystallography. Peptides bind in an extended, but kinked, conformation (9) to a groove on the HLA molecule (16, 17) containing "specificity" pockets formed by polymorphic side chains (11, 18). In a number of different class I MHC molecules, the P2-binding pocket, originally the "B" pocket of HLA-A*0201 (11), is located near the side chain of amino acid 45 of HLA and extends between the α_1 α-helix and the β-sheet that forms the floor of the peptide-binding groove (11, 18). Here we analyze the structure of the P2 specificity pockets of two subtypes of HLA-A and one of HLA-B.†† A steric and chemical match is observed between the specificity pocket and the P2 side chain that it preferentially binds. The shape of the specificity pocket and therefore the selectivity for peptide sequences is seen to depend not only on substitutions of polymorphic positions in the pocket but also on the reorientation of an unsubstituted residue that may be caused by substitutions at remote polymorphic positions in the binding groove. The binding energy contributed by the P2 side chain has been estimated and appears sufficient to explain the observed selectivity of peptide-binding motifs.

The publication costs of this article were defrayed in part by page charge payment. This article must therefore be hereby marked "*advertisement*" in accordance with 18 U.S.C. §1734 solely to indicate this fact.

MATERIALS AND METHODS

Coordinate Transformations. MHC molecules HLA-A*0201, HLA-A*6801, and HLA-B*2705 were superimposed pairwise by the use of transformation matrices determined by a least-squares fit of C^α atoms of amino acids forming the β-sheet of the MHC binding cleft (defined as in ref. 11), achieved with the program WHAFITCA (written by S. J. Remington and M. A. Saper). The structure of influenza virus nucleoprotein peptide Np-(91–99) was transformed from the 2.8-Å resolution structure of HLA-A*6801/Np-(91–99) (15) to the 1.9-Å structure of HLA-A*6801 complexed with a collection of endogenous peptides (PDB1HSB) by using the least-squares transformation based on all C^α atoms in the α_1 and α_2 domains.

Cavity Surface Areas. Cavity surface areas (19) were calculated with the program MS (20) using the parameters described (19). Some bound water molecules contribute to cavity surfaces in HLA-A*6801 and HLA-B*2705.

Contact Atoms. van der Waals contacts were analyzed with the program ACCESS (written by M. D. Handschumacher and F. M. Richards). MHC atoms were considered to contact the peptide if their solvent-accessible surface area (21) with 0.01-Å radius probe differed in the presence or absence of the peptide P2 side-chain atoms, as described (10).

RESULTS

The contact surface of the pocket contacting a P2 side chain has been determined in HLA-A*6801 from x-ray coordinates of a complex with a single peptide refined to 2.8-Å resolution (15) and with a collection of endogenous peptides to 1.9-Å resolution (Fig. 1*A*). Similar contact surfaces were determined from coordinates of HLA-A*0201 refined to 2.6 Å (11)

Abbreviation: MHC, major histocompatibility complex.

‡Present address: Brandeis University, Rosenstiel Research Center, 415 South Street, Waltham, MA 02254.
§Present address: Department of Pediatrics, Children's Hospital of Pittsburgh, 6130 Rangos Research Building, 3705 Fifth Avenue, Pittsburgh, PA 15213.
‖To whom reprint requests should be addressed.

††The atomic coordinates have been deposited in the Protein Data Bank, Chemistry Department, Brookhaven National Laboratory, Upton, NY 11973 (references PDB1HSB, PDB3HLA, and PDB1HSA).

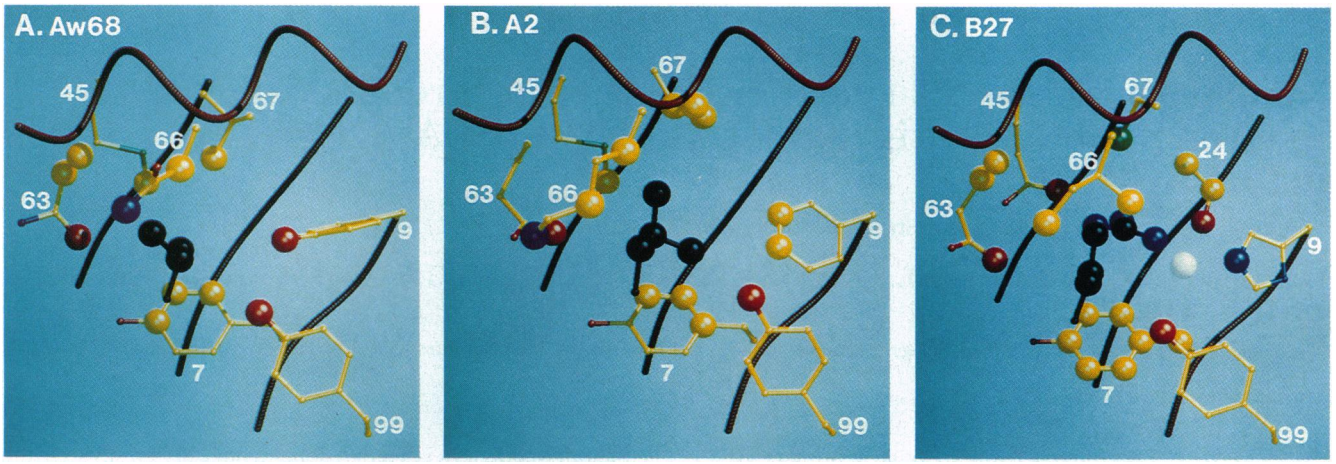

FIG. 1. P2 pockets: Residues that contact the peptide P2 side chain. (*A*) HLA-A*6801, P2 Val contacts. (*B*) HLA-A*0201, P2 Leu contacts. (*C*) HLA-B*2705, P2 Arg contacts. P2 side-chain carbon atoms are shown in black; red spline shows C^{α} atoms of α_1-domain α-helix and β-sheet; contact atoms (see Table 1) are enlarged; oxygen atoms are in red, nitrogen in blue, and carbon in yellow. The figure was generated with HYDRASTER [modified by S. Watowich & L. Gross from programs written by D. Bacon and W. Anderson (RASTER3D) and R. Hubbard (HYDRA)].

and of HLA-B*2705 refined to 2.1 Å (10), both complexed with collections of endogenous peptides (Fig. 1 *B* and *C*). In all three HLA subtypes, seven side chains (residues 7, 9, 45, 63, 66, 67, and 99) form the contact surface of the P2 pocket, with one additional side chain (residue 24) contributing in HLA-B*2705 (Table 1). Two of the contact residues, 7 and 99, are tyrosines that are similarly positioned in all three structures. The contact atom of residue 63, a side-chain oxygen, is also similarly positioned in all three structures, but contributed by different side chains: Asn in HLA-A*6801 and Glu in HLA-A*0201 and HLA-B*2705 (Fig. 1). Two positions have different amino acids in each subtype: 9 (Tyr, Phe, and His in HLA-A*6801, -A*0201, and -B*2705) and 66 (Asn, Lys, and Ile) and two have the same amino acid in the HLA-A isotypes but a different one in the HLA-B isotype: 45 (Met and Glu), 67 (Val and Cys) (Fig. 1 and Table 1).

The peptide sequence preferences of HLA-A*0201, HLA-A*6801, and HLA-B*2705 have been analyzed by Edman degradation and mass spectrometry (5, 7, 8, 23–25). All three class I molecules restrict the sequences of bound peptides at P2, but they select different side chains: a small residue (Val or Thr) for HLA-A*6801, a nonpolar residue (Leu, Ile, or Met) for HLA-A*0201, and a large positively charged residue (Arg) for HLA-B*2705. Other sequence restrictions are observed at P1, P3, and P9.

HLA-B*2705 Specificity. The most notable difference among the three subtypes compared is that the two HLA-A subtypes have a nonpolar, methyl group from Met-45 at the base of the pocket whereas HLA-B*2705 has a negatively charged carboxylate from Glu-45. The carboxylate oxygen ($O^{\epsilon 1}$), along with $O^{\gamma 1}$ of Thr-24 and a water molecule hydrogen-bonded to His-9, is positioned to allow the formation of a planar network of hydrogen bonds to the guanidinium group of a P2 arginine (Fig. 1*C* and ref. 10). The δ-methyl group of Met-45 in the HLA-A subtypes forms nonpolar, van der Waals contacts with P2 methyl groups of Val or Thr in HLA-A*6801 or Leu in HLA-A*0201 (Table 1). HLA-A*6801 can accommodate P2 Thr by forming a hydrogen bond from $O^{\delta 1}$ of Asn-63 to $O^{\gamma 1}$ of P2 Thr (15).

Several polar atoms are found in the P2 pockets of all three class I molecules and form van der Waals contacts, primarily with P2 carbon atoms. However, all these polar atoms make hydrogen bonds within the protein or to solvent or polar peptide main-chain atoms (Table 1). In HLA-B*2705, one water molecule contributes to the surface of the P2 pocket but is also hydrogen-bonded to two MHC side chains (His-9 and Tyr-99) and to another water molecule.

HLA-A*0201 vs. HLA-A*6801 Selectivity. The different specificities of the P2-binding pockets in HLA-A*6801 and HLA-A*0201 depend primarily on steric, rather than chemical, changes within the pocket. Residue 67, which is Val in both molecules, adopts two different side chain conformations. In HLA-A*6801, the Val-67 side chain is in the "minus" ($\chi_1 = -63°$) rotamer conformation (26) where one methyl group blocks deeper access (Fig. 2*A*). In HLA-A*0201, Val-67 is in the "plus" ($\chi_1 = +71°$) rotamer conformation with both methyl groups rotated out of the path of a peptide P2 side chain (Fig. 2*B*), which allows larger side chains such as Leu, Ile, and Met to be accommodated. The $C^{\delta 2}$ atom of a P2 Leu in HLA-A*0201 packs close to the end of Phe-9, in space that is occupied in HLA-A*6801 by the hydroxyl group of Tyr-9. Two other side chains in the P2-binding pocket differ between HLA-A*0201 and HLA-A*6801, 63 (Glu → Asn) and 66 (Lys → Asn) but do not constrict the pocket near the γ-methyl groups of a P2 Leu side chain. These observations suggest that either a Phe-9 → Tyr substitution or a helix shift leading to reorientation of Val-67 (see below) could independently cause the observed change in the specificity of the P2 pocket.

Shift of α_1-Domain α-Helix. The difference in the conformation of the Val-67 side chain appears not to be caused by amino acid differences between HLA-A*6801 and HLA-A*0201 in the P2 pocket (such as Tyr/Phe-9) but instead to be primarily due to a concerted shift of the α_1-domain α-helix along its axis by about 0.7 Å (Fig. 3), so that the Val-67 rotamer of HLA-A*0201 is sterically hindered in HLA-A*6801. Although the magnitude of this structural difference is near the coordinate error for the two structures, when the eight-stranded β-sheets of the α_1 and α_2 domains are superimposed by least-squares fit, both those sheets and the α_2-domain α-helices overlap with small rms residuals (0.33 and 0.46) and no systematic deviations in x, y, or z, as expected (Table 2). In contrast, the α_1-domain α-helices (residues 50–84) have a rms residual almost twice as large (0.76) and systematic deviations along x and y with mean values of 0.56 and 0.44 Å, 10 times those seen with the α_2-domain α-helices (Table 2). The approximate x and y coordinate directions are shown in Fig. 3, where it is evident that the α_1-domain α-helix in HLA-A*0201 is shifted toward its N terminus relative to that of HLA-A*6801. Differences in the α_1-domain α-helices are also observed between HLA-A*6801 and HLA-B*2705, but the direction is different (Table 2) with the HLA-B*2705 helix shifted slightly away from the α_2 α-helix and toward the β-sheet (figure not shown). Al-

Table 1. Contacts between MHC atoms and P2 side-chain atoms

MHC residue			P2 atom(s)		
No.	Identity	Atom	A*6801/Val	A*0201/Leu	B*2705/Arg
7	Tyr	C^{β}	—	—	$N^{\eta 1}$
		C^{γ}	—	$C^{\delta 2}$	C^{γ}
		$C^{\delta 1}$	—	—	C^{γ}
		$C^{\varepsilon 1}$	—	—	C^{γ}
		$C^{\delta 2}$	C^{β}, $C^{\gamma 1}$	C^{γ}, $C^{\delta 2}$	C^{γ}, C^{δ}, N^{ε}, C^{ζ}, $N^{\eta 1}$, $N^{\eta 2}$
		$C^{\varepsilon 2}$	C^{β}, $C^{\gamma 1}$	C^{γ}, $C^{\delta 2}$	C^{γ}, C^{δ}, N^{ε}, C^{ζ}, $N^{\eta 1}$, $N^{\eta 2}$
		C^{ζ}	$C^{\gamma 1}$	—	C^{γ}
9	Tyr	O^{η}	C^{β}		
	Phe	$C^{\varepsilon 2}$		$C^{\delta 2}$	
		C^{ζ}		$C^{\delta 2}$	
	His	$N^{\varepsilon 2}$			$N^{\eta 1}$
24	Thr	C^{β}			$N^{\eta 1}$
		$O^{\gamma 1}$			$\underline{N}^{\eta 1}$, $N^{\eta 2}$
		$C^{\gamma 2}$			C^{ζ}, $N^{\eta 1}$, $N^{\eta 2}$
45	Met	C^{ε}	C^{β}, $C^{\gamma 1}$, $C^{\gamma 2}$	C^{γ}, $C^{\delta 1}$, $C^{\delta 2}$	
	Glu	$O^{\varepsilon 1}$			C^{δ}, $\underline{N}^{\varepsilon}$, C^{ζ}, $\underline{N}^{\eta 2}$
63	Asn	C^{α}	$C^{\gamma 2}$		
		C^{β}	$C^{\gamma 2}$		
		$O^{\delta 1}$	$C^{\gamma 2}$		
	Glu	C^{α}		—	C^{δ}
		C^{β}		—	C^{δ}
		$O^{\varepsilon 1}$		C^{β}, C^{γ}	C^{β}, C^{γ}
66	Asn	C^{β}	$C^{\gamma 2}$		
		$N^{\delta 2}$	$C^{\gamma 2}$		
	Lys	C^{β}		$C^{\delta 1}$	
		C^{δ}		C^{β}	
		N^{ζ}		C^{β}	
	Ile	$C^{\gamma 2}$			C^{β}, C^{δ}
		$C^{\delta 1}$			C^{β}
67	Val	N	—	$C^{\delta 1}$	
		C^{α}	—	$C^{\delta 1}$	
		C^{β}	—	$C^{\delta 1}$	
		$C^{\gamma 1}$	C^{β}, $C^{\gamma 1}$, $C^{\gamma 2}$	—	
		$C^{\gamma 2}$	—	$C^{\delta 1}$	
	Cys	S^{γ}			C^{δ}, N^{ε}, C^{ζ}, $N^{\eta 1}$, $N^{\eta 2}$
99	Tyr	O^{η}	C^{β}, $C^{\gamma 1}$	$C^{\delta 2}$	C^{β}, C^{γ}

Only atoms in contact are listed. —, No contact atom; blank, not relevant; underlined atoms, hydrogen bonds (<3.2 Å) to MHC side chain. Nomenclature for side-chain atoms is in ref. 22.

though we cannot explain this structural difference between the two HLA-A subtypes in terms of specific amino acid substitutions, it may be a result of amino acid differences between HLA-A*0201 and HLA-A*6801 at polymorphic positions (residues 70, 74, 95, 97, 114, and 116) at the "right-hand end" of the groove (Fig. 3). The net effect of these remote polymorphic differences would then be to alter the shape of the P2 pocket by shifting the α_1 α-helix and inducing a change in the conformation of Val-67.

Peptide Binding Energy. In these structures, the P2 side chain of a bound peptide is packed tightly among the MHC side chains that form its binding pocket. The stabilization of a protein's native folded conformation by side chains packed in hydrophobic cores has been studied in T4 lysozyme (19), and the stabilization energy ($\Delta\Delta G_{fold}$) has been modeled as the sum of the side chain's free energy of transfer from water to an organic solvent (desolvation) (28, 29) and the molecular surface area of the cavity occupied by the side chain (dispersion forces) (19). Both terms are evaluated relative to a putative replacement side chain. An alternative interpretation in terms of the work of cavity formation in the solvent and in the protein interior predicts that the stabilization energy lies between the desolvation energy difference (minimum) and the energy of cavity formation in water necessary to accommodate the larger side chain (maximum) (30). We have performed analogous calculations on the P2 side chain bound in its specificity pocket, relative to a Gly replacement side chain. Neglecting the entropic effects of peptide main-chain torsional flexibility, a peptide with P2 Val should bind HLA-A*6801 more tightly than a peptide with P2 Gly by ≈3.0 kcal·mol^{-1} [≈1.7 kcal·mol^{-1} (desolvation) + ≈1.3 kcal·mol^{-1} (66-Å^2 cavity surface area times 20 cal·mol^{-1}·Å^{-2})]. For a P2 Leu complexed with HLA-A*0201, the differential binding energy relative to Gly would be ≈4.5 kcal·mol^{-1} [≈2.5 kcal·mol^{-1} (desolvation) + ≈2.0 kcal·mol^{-1} (98-Å^2 cavity surface area)]. Our calculations cannot account for side-chain repacking and therefore may overestimate the differential binding energy (19, 30). Nevertheless, the desolvation term can be taken as a minimum estimate (30). This analysis cannot be extended to the P2 Arg anchor of HLA-B*2705, because of the presence of several hydrogen bonds. Uncharged hydrogen bonds generally stabilize binding by 0.5–2.0 kcal·mol^{-1}, while ones with poor geometry can destabilize binding by 0.5 kcal·mol^{-1}; hydrogen bonds involving a buried, charged atom appear to stabilize binding by 3.0–4.5 kcal·mol^{-1} (31, 32). Since the geometry of the uncharged hydrogen bonds between P2 Arg and HLA-B*2705 is reasonable, the P2 Arg hydrogen bonds are likely to contribute >3.0 kcal·mol^{-1} to the binding energy of the peptide. In addition, binding of the aliphatic moiety of the Arg side chain probably adds to the binding energy, but its effect cannot be estimated directly from the cavity surface area (137 Å^2)

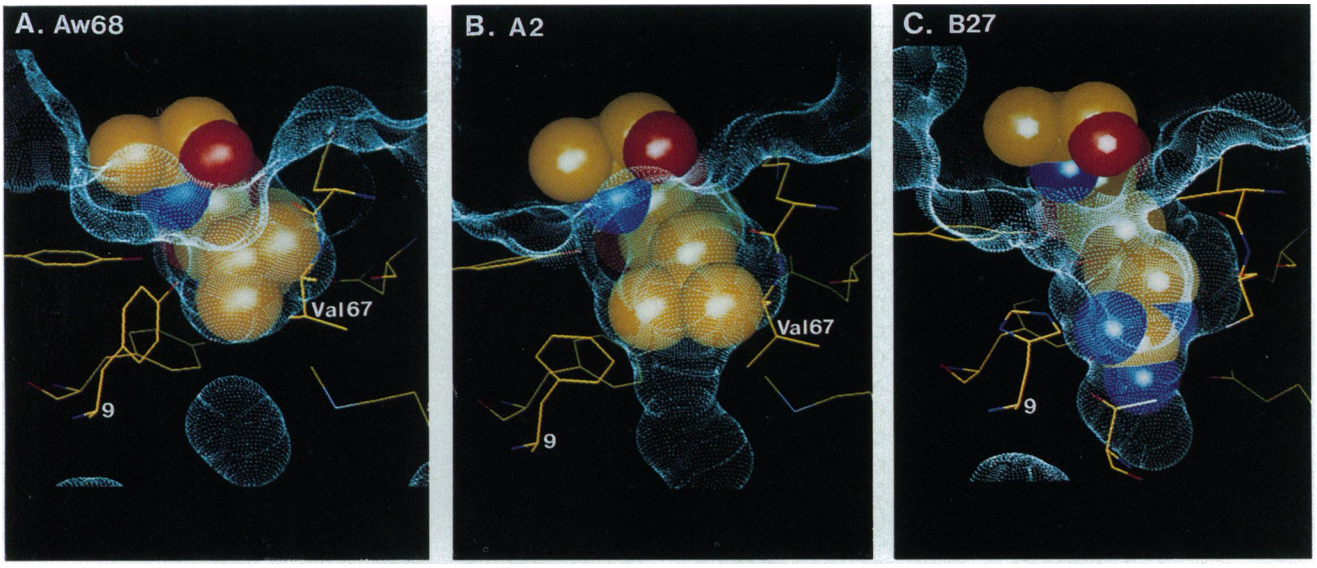

FIG. 2. Shape of P2 pockets. (*A*) HLA-A*6801 with Val. (*B*) HLA-A*0201 with Leu. (*C*) HLA-B*2705 with Arg. Solid surface, van der Waals surface of peptide; red, oxygen; blue, nitrogen; yellow, carbon; dot surface, molecular surface (20, 27) of MHC molecule. The figure was prepared with INSIGHT II (Biosym Technologies, San Diego) according to the user guide for Version 2.1.0.

because the van der Waals interactions of the polar atoms are included in the hydrogen-bond measurements (19, 30). Nevertheless, the potential energetic contribution of P2 Arg compared with P2 Gly is likely to be larger than that estimated from hydrogen-bonding interactions alone.

DISCUSSION

Class I histocompatibility glycoproteins bind mostly short peptides (1, 5, 7, 8, 25) in an extended conformation with a kink near P4 (9, 10, 12–15), although cases have been described of bound octapeptides slightly straightened at the kink (12, 14) and of deca- to tridecapeptides that probably bulge at their centers (8, 23, 24). Histocompatibility antigens interact very specifically with the side chains of peptides at only a few positions of the peptide sequence ("anchors") (9), through pockets in the peptide-binding groove (11, 18). Peptide anchor side chains often occur near the ends of the peptide at P2 or P3 and PΩ, as is found for HLA-A*0201, HLA-A*6801, and HLA-B*2705. However, one anchor in H-2K^b is at P(Ω − 3). In each case, other side chains (e.g., P1, P6, and P7 in the HLA-A*6801/nucleoprotein peptide complex) also contact the HLA molecule but do not appear constrained by a very specific pocket. Fig. 4 shows the influenza virus nucleoprotein peptide Np-(91–99) (KTGG-PIYKR) bound to HLA-A*6801, where the two "anchor" positions P2 (Thr) and P9 (Arg) are clearly buried in pockets in the groove, but P3 (Gly), P5 (Pro), and P6 (Ile) also contact the site (15). Parts of P1 and P4–P8 are accessible to solvent at the HLA surface and therefore presumably available for direct recognition by T-cell receptors (15).

Conserved sites at both ends of the peptide-binding groove interact with the peptide N and C termini and main chain in all class I/peptide complexes studied to date (8–10, 12–15, 33). Elsewhere, we have argued that the binding of the peptide main chain (class I and class II) and termini (class I) provides the dominant interactions of peptide with MHC molecules (8, 10, 15, 33, 34), consistent with experiments with truncated or extended peptides (refs. 35 and 36; A. Sette, unpublished work). Since anchor side chains are generally a fixed distance from the N or C terminus in class I-associated peptides, their binding is presumably coupled to that of the associated terminus (8, 23–25). An incorrect peptide anchor side chain that cannot be accommodated in its

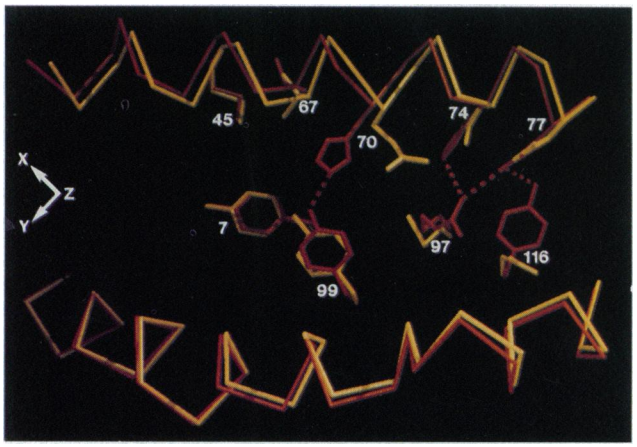

FIG. 3. Superposition of A subtypes to show shifts in α_1-domain α-helix and altered Val-67 conformation. HLA-A*0201 is in red and HLA-A*6801 in yellow. Dotted lines show hydrogen bonds. See also Table 2 and text. The figure was prepared with HYDRASTER (see legend to Fig. 1).

Table 2. $\alpha_1\alpha_2$ domain superposition by β-sheet C$^\alpha$ positions

		Aw68/A2	Aw68/B27
β-sheet	Δrms	0.33	0.35
	⟨Δx⟩	0.00	0.00
	⟨Δy⟩	0.00	0.00
	⟨Δz⟩	0.00	0.00
α_2 α-helix	Δrms	0.46	0.44
	⟨Δx⟩	−0.05	−0.04
	⟨Δy⟩	−0.02	−0.04
	⟨Δz⟩	0.07	0.02
α_1 α-helix	Δrms	0.76	0.66
	⟨Δx⟩	0.56	0.41
	⟨Δy⟩	0.44	−0.12
	⟨Δz⟩	−0.26	−0.41

Aw68, HLA-A*6801; A2, HLA-A*0201; B27, HLA-B*2705; root-mean-square deviation (Δrms) = $[\Sigma(\Delta x^2 + \Delta y^2 + \Delta z^2)/n]^{1/2}$; $\langle\Delta x\rangle = \Sigma\Delta x/n$; $\langle\Delta y\rangle = \Sigma\Delta y/n$; $\langle\Delta z\rangle = \Sigma\Delta z/n$. The *x*, *y*, and *z* approximate directions and superposition are shown in Fig. 3. Significant *x*, *y*, and *z* shifts in the α_1 α-helix are underlined.

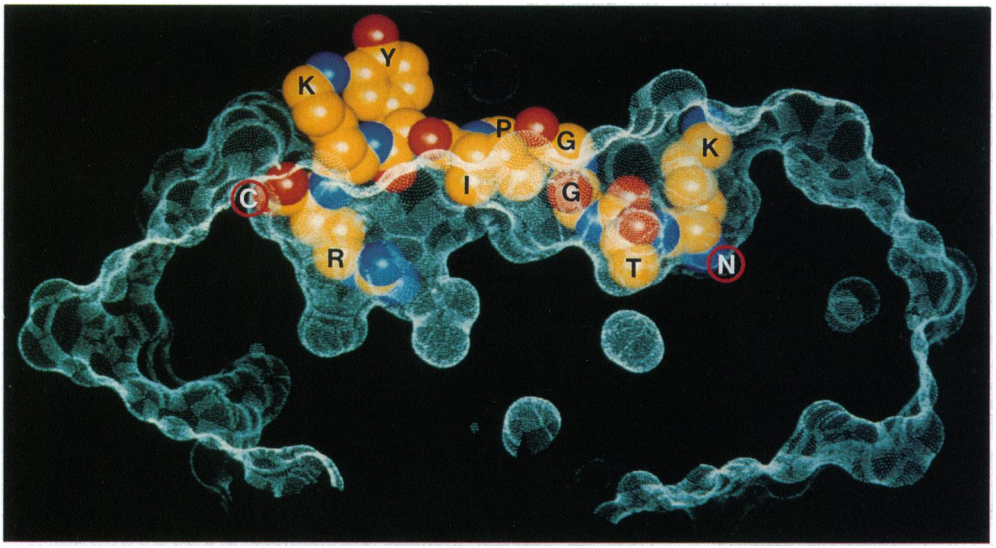

FIG. 4. Influenza virus nucleoprotein peptide Np-(91–99) (KTGGPIYKR) bound to HLA-A*6801, showing P2 Thr and P9 Arg buried in specificity pockets. Solid surface shows van der Waals surface of peptide labeled by single-letter amino acid code; N- and C-terminus labels are white circled by red. Dot surface shows molecular surface (20, 27) of HLA-A*6801. The figure was prepared with INSIGHT II (see Fig. 2 legend). Six water molecules inside the binding cleft were left out in generating the molecular surface.

specificity pocket (based on size or charge) may disrupt not only the anchor's binding but also that of the nearby terminus, drastically reducing the peptide's affinity for the MHC molecule. However, if the anchor side chain were suboptimal but could still be accommodated, only the anchor's binding energy would be affected.

Here we have estimated the energy of binding of optimal peptide P2 side chains to the P2-binding pockets of three class I molecules and suggest that they may contribute several kilocalories per mole (relative to Gly). Since $\Delta\Delta G \approx 1.4$ kcal·mol^{-1} corresponds to a 10-fold decrease in the equilibrium dissociation constant, the optimal P2 side chain could confer binding several orders of magnitude tighter compared with a small, incorrect side chain, thus explaining the preponderance of bound peptides that fulfill a given class I MHC molecule's binding motif. The analysis also shows that the shapes and therefore specificities of the pockets may be determined by substitutions remote from the pocket, which alter the conformation of an unsubstituted residue, Val-67. This result suggests caution in predicting "anchor" residues from the sequences of class I molecules for which structures are not known.

Peptide binding may be further modulated by other side chains, as observed for class II-binding peptides (34). In class I/peptide complexes, several peptide side chains contact nonspecific MHC pockets (e.g., P3 and P7 in HLA-B*2705) but appear to be only loosely constrained (7, 9). Steric or electrostatic incompatibility of these "secondary anchors" could block binding both locally and at nearby pockets, while a particularly advantageous peptide side chain might provide a significant increase in stabilization. Evidence for such effects by "secondary anchor" side chains has been found for peptides in HLA-A*0201 (37) and HLA-DR1 (34).

We acknowledge the earlier contributions of T. P. J. Garrett, M. A. Saper, and P. J. Bjorkman to this project, the technical assistance of Anastasia Haykov and Polina Klimovitsky and computation time provided by the Pittsburgh Supercomputer Center. H.-C.G. is a Cancer Research Institute Fellow and D.R.M. is supported by a National Institutes of Health training grant. J.C.G. is supported by a Career Development Award from the Juvenile Diabetes Foundational International. J.L.S. acknowledges support from the National Institutes of Health. D.C.W. is an Investigator of the Howard Hughes Medical Institute.

1. Rötzschke, O., Falk, K., Deres, K., Schild, H., Norda, M., Metzger, J., Jung, G. & Rammensee, H.-G. (1990) *Nature (London)* **348**, 252–254.
2. Townsend, A. R. M., Gotch, F. M. & Davey, J. (1985) *Cell* **42**, 457–467.
3. Townsend, A. & Bodmer, H. (1989) *Annu. Rev. Immunol.* **7**, 601–624.
4. Lawlor, D. A., Zemmour, J., Ennis, P. D. & Parham, P. (1990) *Annu. Rev. Immunol.* **8**, 23–63.
5. Falk, K., Rötzschke, O., Stevanovic, S., Jung, G. & Rammensee, H.-G. (1991) *Nature (London)* **351**, 290–296.
6. Van Bleek, G. M. & Nathenson, S. G. (1991) *Proc. Natl. Acad. Sci. USA* **88**, 11032–11036.
7. Jardetzky, T. S., Lane, W. S., Robinson, R. A., Madden, D. R. & Wiley, D. C. (1991) *Nature (London)* **253**, 326–329.
8. Guo, H.-C., Jardetzky, T. S., Garrett, T. P. J., Lane, W. S., Strominger, J. L. & Wiley, D. C. (1992) *Nature (London)* **360**, 364–366.
9. Madden, D. R., Gorga, J. C., Strominger, J. L. & Wiley, D. C. (1991) *Nature (London)* **353**, 321–325.
10. Madden, D. R., Gorga, J. C., Strominger, J. L. & Wiley, D. C. (1992) *Cell* **70**, 1035–1048.
11. Saper, M. A., Bjorkman, P. J. & Wiley, D. C. (1991) *J. Mol. Biol.* **219**, 277–319.
12. Fremont, D. H., Matsumura, M., Stura, E. A., Peterson, P. A. & Wilson, I. A. (1992) *Science* **257**, 919–927.
13. Matsumura, M., Fremont, D. H., Peterson, P. A. & Wilson, I. A. (1992) *Science* **257**, 927–934.
14. Zhang, W., Young, A. C. M., Imarai, M., Nathenson, S. G. & Sacchettini, J. C. (1992) *Proc. Natl. Acad. Sci. USA* **89**, 8403–8407.
15. Silver, M. L., Guo, H.-C., Strominger, J. L. & Wiley, D. C. (1992) *Nature (London)* **360**, 367–369.
16. Bjorkman, P. J., Saper, M. A., Samraoui, B., Bennett, W. S., Strominger, J. L. & Wiley, D. C. (1987) *Nature (London)* **329**, 506–512.
17. Bjorkman, P. J., Saper, M. A., Samraoui, B., Bennett, W. S., Strominger, J. L. & Wiley, D. C. (1987) *Nature (London)* **329**, 512–518.
18. Garrett, T. P. J., Saper, M. A., Bjorkman, P. J., Strominger, J. L. & Wiley, D. C. (1989) *Nature (London)* **342**, 692–696.
19. Eriksson, A. E., Baase, W. A., Zhang, X.-J., Heinz, D. W., Blaber, M., Baldwin, E. P. & Matthews, B. W. (1992) *Science* **255**, 178–183.
20. Connolly, M. L. (1983) *J. Appl. Crystallogr.* **16**, 548–558.
21. Lee, B. & Richards, F. M. (1971) *J. Mol. Biol.* **55**, 379–400.
22. Anonymous (1970) *J. Mol. Biol.* **52**, 1–17.
23. Wei, M. & Cresswell, P. (1992) *Nature (London)* **356**, 443–446.
24. Henderson, R. A., Michel, H., Sakaguchi, K., Shabanowitz, J., Appella, E., Hunt, D. F. & Engelhard, V. H. (1992) *Science* **255**, 1264–1266.
25. Hunt, D. F., Henderson, R. A., Shabanowitz, J., Sakaguchi, K., Michel, H., Sevilir, N., Cox, A. L., Appella, E. & Engelhard, V. H. (1992) *Science* **255**, 1261–1263.
26. Ponder, J. W. & Richards, F. M. (1987) *J. Mol. Biol.* **193**, 775–791.
27. Richards, F. M. (1977) *Annu. Rev. Biophys. Bioeng.* **6**, 151–176.
28. Damodaran, S. & Song, K. B. (1986) *J. Biol. Chem.* **261**, 7220–7222.
29. Fauchère, J.-L. & Pliska, V. (1983) *Eur. J. Med. Chem.* **18**, 369–375.
30. Lee, B. (1993) *Protein Sci.* **2**, 733–738.
31. Fersht, A. R., Shi, J.-P., Snill-Jones, J., Lowe, D. M., Wilkinson, A. J., Blow, D. M., Brick, P., Carter, P., Waye, M. M. Y. & Winter, G. (1985) *Nature (London)* **314**, 235–238.
32. Serrano, L., Kellis, J. T., Jr., Cann, P., Matouschek, A. & Fersht, A. R. (1992) *J. Mol. Biol.* **224**, 783–804.
33. Madden, D. R. & Wiley, D. C. (1992) *Curr. Opin. Struct. Biol.* **2**, 300–304.
34. Jardetzky, T. S., Gorga, J. C., Busch, R., Rothbard, J., Strominger, J. L. & Wiley, D. C. (1990) *EMBO J.* **9**, 1797–1803.
35. Cerundolo, V., Elliott, T., Elvin, J., Bastin, J., Rammensee, H.-G. & Townsend, A. (1991) *Eur. J. Immunol.* **21**, 2069–2075.
36. Tsomides, T. J., Walker, B. D. & Eisen, H. N. (1991) *Proc. Natl. Acad. Sci. USA* **88**, 11276–11280.
37. Ruppert, J., Sidney, J., Celis, E., Kubo, R. T., Grey, H. M. & Sette, A. (1993) *Cell*, in press.